Journal of Inorganic Biochemistry 195 (2019) 71–82

Contents lists available at ScienceDirect

Journal of Inorganic Biochemistry

journal homepage: www.elsevier.com/locate/jinorgbio

Phleomycin complex – Coordination mode and in vitro cleavage of DNA

Kamila Stokowa-Sołtys*, Valentyn Dzyhovskyi, Robert Wieczorek, Małgorzata Jeżowska-Bojczuk[1]

Faculty of Chemistry, University of Wroclaw, F. Joliot-Curie 14, 50-383 Wroclaw, Poland

A B S T R A C T

Phleomycin is one of the anticancer glycopeptide antibiotics which cause DNA cleavage. It is commonly used as a copper(II) complex. Therefore, it is important to study the metal ion binding process and to define the coordination mode. In this paper, we describe the acid-base properties of phleomycin and the coordination sphere of the Cu(II) cation. In the metal binding process up to five nitrogen donor atoms can be involved. Four of them in the same plane deriving from: the pyrimidine ring, secondary amine of β-aminoalanine, imidazole and amide of the nearest peptide bond (from β-hydroxyhistidine) and in the apical position from the α-amino functional group of β-aminoalanine, resulting complex has a square-pyramidal geometry. Phleomycin complexes are able to induce single- and double-stranded DNA damage when they are accompanied by one-electron reductants, such as dithiothreitol, glutathione, 2-mercaptoethanol or ascorbic acid. In such conditions they produce reactive oxygen species which are responsible for DNA cleavage. The metal ion binding site is relatively close to the nucleic acid interacting moiety. This supports the hypothesis that copper ion is important in the anticancer activity which involves DNA degradation.

1. Introduction

Cancer constitutes an enormous burden on all societies [1]. In recent years, the number of new cases have continued to increase, largely because of the aging and growth of the world population [2]. This situation is more and more frequently referred to as an “epidemic”. Cancer is now one of the leading causes of morbidity and mortality worldwide, with estimated 18.1 million new cases and almost 9.6 million deaths in 2018 [3]. All over the world, about 1 in 6 deaths is due to cancer. It is predicted that by 2030, the number of new cases of cancer will increase to 10–11 million each year in low and middle economically developed countries alike. At the same time, cancer-related deaths will increase to 13 million per year. In 2018, the most common causes of cancer death were lung, liver, stomach, colorectal and prostate cancers in male population. Five most frequent types of cancer in women are breast, lung, colorectal, cervical and stomach cancers [4]. In many cases, human microbiota is associated with cancer progression, e.g. *Helicobacter pylori* is related to stomach cancer [5], *Fusobacterium nucleatum* promotes colon cancer growth and even metastasis [6].

Some of the most common cancer types are largely curable, if they are diagnosed at an early stage and adequately treated. Therefore, there is a need to improve diagnostic tools and the methods of treatment [7]. First of all, the understanding of the mechanism of action of anticancer drugs at the molecular level is essential. Some of the natural glycopeptide antibiotics like bleomycin are widely used during therapy. It is commonly believed that they have a biological effect similar to that of metallodrugs [8]. Metal ion is crucial in the mode of action and it is responsible for the oxidative damage of DNA [9].

The first studies on the coordination process of different metal ions by bleomycin were performed in the 1970s [10]. However, the topic has been recurring in the literature for the following several decades [11–19]. Researchers have not agreed when it comes to the number, arrangement and nature of donor atoms. While the involvement of the imidazole, pyrimidine and secondary amino group seems to be indisputable during metal binding, other donor atoms have still been controversial. The structure of the complex could become more clear if the X-ray structure were solved. Unfortunately, the crystals have been obtained only for the cupric complexes with bleomycin derivatives – a product of the biosynthesis of bleomycin and its structural analogs. There was a lack of sugar and bithiazole moieties that could be involved in metal binding [20]. Therefore, the complete coordination sphere could not be fully confirmed. Interestingly, on the absorption spectra of Cu(II)-bleomycin and its derivatives, d-d bands have been observed at the wavelength of around 600 nm which suggests the presence of a strong ligand-field in a disordered five or six-coordinate model. The potential involvement of the primary amino group of β-aminoalanine, sugar moieties and bithiazole ring has been widely discussed. In view of the fact that numerous complexes with bleomycin and its synthetic analogs precipitate from the solution, only partial potentiometric and spectroscopic data are reported in the literature [14–19]. It was a starting point to study the interactions of copper(II) ions with phleomycin, bleomycin's structural analog, whose complexes are soluble in the whole pH range. Therefore, it was possible to obtain the full

* Corresponding author.
E-mail address: kamila.stokowa-soltys@chem.uni.wroc.pl (K. Stokowa-Sołtys).
[1] Professor Małgorzata Jeżowska-Bojczuk passed away in 2018.

https://doi.org/10.1016/j.jinorgbio.2019.03.010
Received 16 November 2018; Received in revised form 15 February 2019; Accepted 10 March 2019
Available online 21 March 2019
0162-0134/

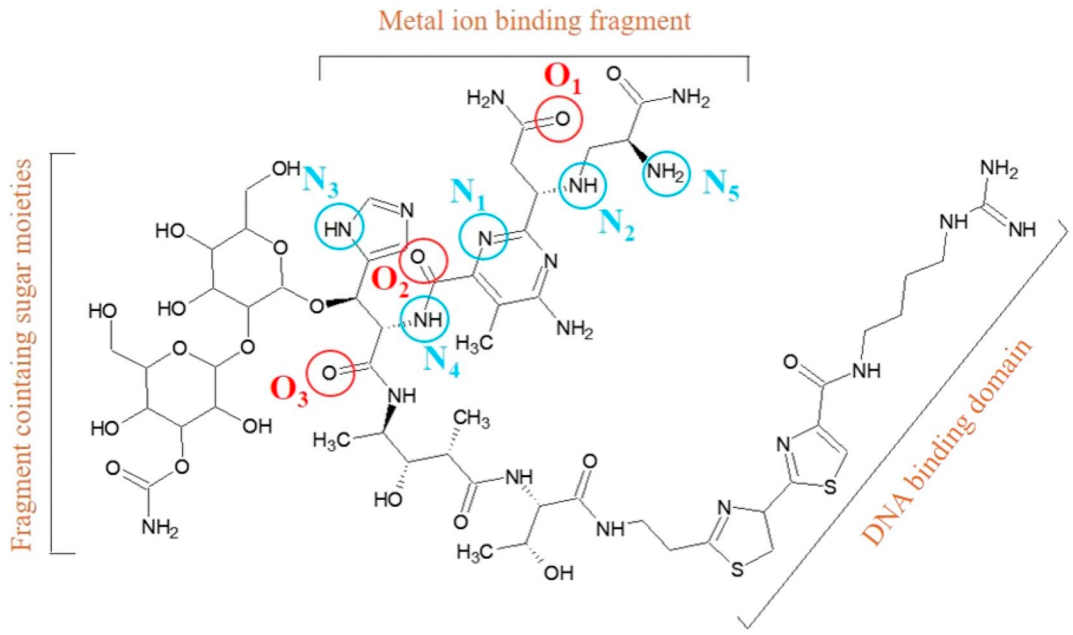

Fig. 1. Molecular structure of phleomycin in its fully deprotonated form.

potentiometric and spectroscopic characteristics of the coordination process. Moreover, the computational results allowed to predict the most stable species.

Phleomycin (Fig. 1) is a glycopeptide antibiotic, member of the bleomycins family isolated for the first time from *Streptomyces verticillus* [21]. This wide-spectrum antibiotic has an anticancer activity which is based on the DNA cleavage. Severe DNA damage leads to cell death [22]. From the structural point of view, phleomycin only slightly differs from bleomycin. It has a thiazinylthiazole moiety in lieu of bithiazole present in bleomycin and it naturally occurs as a copper(II) complex [23]. This structural change does not have any impact on the coordination mode, but it increases the solubility of the compound.

2. Experimental section

2.1. Materials

Phleomycin copper(II) complex as blue powder was purchased from Sigma-Aldrich and used without further purification. The pBR322 plasmid DNA buffered solution and other chemical reagents (like NaOH, HCl) were obtained from commercial sources, mainly from Merck.

2.2. Potentiometric titrations

Potentiometric measurements of phleomycin and its complexes with copper(II) ions in aqueous solution in the constant ionic strength (0.1 M KCl) were performed at 298 K under argon atmosphere using pH-metric titrator (905 Titrando Methrom with a combined glass-Ag/AgCl electrode Metrohm Biotrode). Electrode was calibrated daily in concentration using HCl titrations. The CO_2-free NaOH solution at a concentration of 0.1021 M was used as a titrant. The samples (a total volume of 1.5 mL) were titrated in the pH region 1.5–11.0. Ligand concentration was 1×10^{-3} M, and metal-to-ligand molar ratios of 1:1, 1:3, 2:1 were used. Obtained data were analyzed using the SUPERQUAD program [24]. Standard deviations (σ values) quoted were computed also by SUPERQUAD and refer to random errors only. They are, however, a good indication of the importance of the particular species involved in the equilibria.

2.3. UV–Vis

Absorption spectra were recorded on a Cary 60 spectrophotometer (Agilent Technologies) in the 800–200 nm range, using 0.1 and 1 cm cuvettes. Solutions were in the same concentrations and molar ratios as used in potentiometric studies. All spectra were analyzed with the assumption that the spectrum recorded at a given pH $\varepsilon(\lambda,pH)$, is the weighted average of individual spectra of all species present in the solution, $\varepsilon_i(\lambda)$. The weights, $x_i(pH)$, are molar fractions of individual complexes. Concentrations of the species, $c_i(pH)$ were calculated according to their β values determined by potentiometry.

The measurements of ROS (reactive oxygen species) generation were carried out on the above-mentioned UV–Vis spectrophotometer equipped with Single Cell Peltier Accessory (Agilent Technologies) to achieve constant temperature (37 °C). Experiments were performed in the presence of 0.01 mM phleomycin complex, 1 mM cofactors (H_2O_2, ascorbic acid, dithiothreitol (DTT), 2-mercaptoethanol, glutathione) and reporting molecule *N*,*N*-dimethyl-p-nitrosoaniline (NDMA) as a scavenger for hydroxyl radical (·OH). Bleaching of NDMA characteristic band (= 440 nm) suggest production of assayed radicals.

2.4. Circular dichroism

Circular dichroism (CD) spectroscopy experiments were performed on a spectropolarimeter Jasco J-1500 at 298 K in a 0.1 cm and 1 cm quartz cell. The spectral range was 200–400 and 350–800 nm, respectively. The solutions were prepared in the same manner as for UV–Vis spectroscopy. The direct CD measurements (Θ [mdeg]) were converted to mean residue molar ellipticity ($\Delta\varepsilon$ [$M^{-1}\,cm^{-1}$]) using Jasco Spectra Manager.

2.5. EPR

The 1 mM and 3 mM phleomycin solutions (metal-to-ligand molar ratios of 1:1) for EPR measurements with ethylene glycol (water:glycol, 2:1, v/v) were prepared to ensure homogeneity of frozen samples. The spectra were recorded at 120 K (liquid nitrogen) on a Bruker spectrophotometer (Bruker ELEXSYS E500 CW-EPR) at the X-band frequency (9.5 GHz). All EPR parameters were calculated through spectral simulation in the Doubletnew (EPR OF S = 1/2) as implemented by Dr.

Andrew Ozarowski, National High Field Magnetic Laboratory, University of Florida for the spectra obtained at the maximum concentration of the particular species for which well-resolved components were observed.

2.6. Gel electrophoresis

The ability to induce strand breaks by phleomycin complex in the presence of different reagents which may be involved in the anticancer activity of the drug (e. g. 1,4-dithiothreitol (DTT), 2-mercaptoethanol, glutathione (GSH), H_2O_2 and ascorbic acid) was tested with the pBR322 plasmid DNA using agarose gel electrophoresis. The buffered samples (phosphate buffer, pH 7.4) contained combinations of DNA (0.25 μg/mL) and the components of the investigated systems (final concentrations stated below each electropherogram). After 1 h of incubation at 37C, 4 μL of loading buffer (bromophenol blue in 30% glycerol) was added to the reaction mixtures (20 μL) and then loaded on 1% agarose gels, containing ethidium bromide, in TBE buffer (90 mM Tris-borate, pH 8.0; 20 mM EDTA). Gel electrophoresis was done at a constant voltage of 4 V/cm for 120 min. The gels were photographed and processed with a Digital Imaging System (Syngen Biotech, Wrocław, Poland).

2.7. Computational calculations

Molecular orbital studies on Cu(II) cations with phleomycin 1:1 complex have been done on the DFT (density functional theory) level of theory with IEFPCM [25] solvent (water) model introduced upon potential energy surface investigation. The starting structure of the peptide for DFT calculations was generated on the basis of the amino acid sequence after 75 ps simulation at 300 K, without cutoffs using BIO + implementation of CHARMM force field. The DFT calculations on all complexes were performed with Gaussian 09C.01 [26] suite of programs using the M06-2× [27] hybrid functional and 6-31G basis set.

3. Results and discussion

Phleomycin was isolated as a light blue copper(II) complex in 1959 [28], and it has been commercially available in such form until today. The average Cu(II) content is around one metal ion per 3.44 phleomycin molecules [29]. Therefore, in order to determine the deprotonation constants of the ligand itself, it was necessary to remove cupric ions from the complex. To this end, Chelex® 100 chelating resin was applied. This styrene divinylbenzene copolymer contains paired iminodiacetate ions which act as chelating groups in the polyvalent metal ions binding. The effectiveness of the applied method was confirmed by the vanishing of signals in EPR spectra. A complete removal of the copper(II) ions was observed after double treatment of the antibiotic solution with Chelex® (0.25 g of the resin per 5 mL of the antibiotic solution) and incubation with gentle stirring at room temperature for 1 h.

The above-mentioned procedure allowed to perform potentiometric

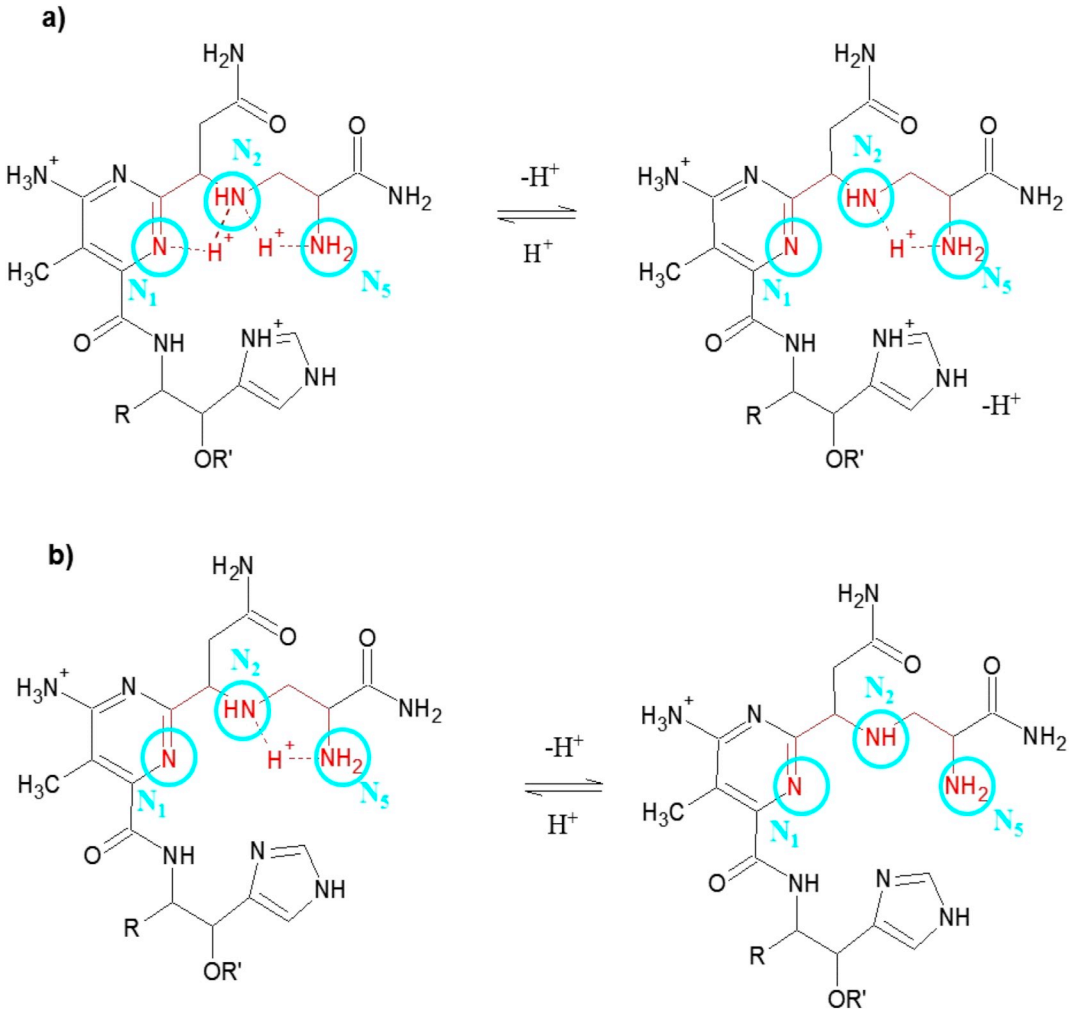

Fig. 2. The scheme of two deprotonation processes occurring in a phleomycin molecule a) in the part of pyrimidine derivative; b) amino group. R and R' reflect to the substituents neglected in the molecular structure of the drug.

Table 1
Potentiometric and spectroscopic parameters for the uncomplex phleomycin.

Potentiometry			UV–Vis		CD	
Ligand	logβ[a]	pK_a[b]	λ [nm]	ε [$M^{-1}cm^{-1}$]	λ [nm]	Δε [$M^{-1}cm^{-1}$]
H_7L^{7+}	42.012(5)	1.69	243	3688	210	+0.670
			300	1555	235	−0.249
H_6L^{6+}	40.324(4)	1.77				
H_5L^{5+}	38.552(5)	2.66				
H_4L^{4+}	35.892(6)	6.38				
H_3L^{3+}	29.511(7)	7.12				
H_2L^{2+}	22.388(5)	11.19				
HL^{+}	11.195(9)	11.20	243	3695	210	+0.100
			300	1563	240	−0.032

Standard deviations on the last digit of stability constants are given in parentheses.

[a] Overall stability constants (β) expressed by the equation: $\beta(H_nL^{n+}) = [H_nL^{n+}]/[L][H^+]^n$).

[b] Acid dissociation constants (pK_a) expressed by: $pK_a = \log\beta(H_nL^{n+}) - \log\beta(H_{n-1}L^{(n-1)+})$.

titrations of the ligand and the complex. Therefore, the overall stability constants for the tested system could be obtained. However, when considering the number of deprotonating groups while increasing the pH value, it should be stressed that three moieties which are potentially able to release protons are engaged in the intramolecular hydrogen bonds (HBs) formation. HBs are created between the heterocyclic nitrogen atom of pyrimidine derivative (N_1 in Figs. 1 and 2) and secondary (N_2, Figs. 1 and 2) and primary (N_5, Figs. 1 and 2) amino groups. Such a HBs network leads to the formation of two stable, five-membered chelate rings. This structural arrangement is able to release only two protons, instead of three as it might be expected. Moreover, neither amide nitrogen atoms nor hydroxyl groups release protons (pK_a value > 13) [30,31]. Consequently, phleomycin behaves like a heptaprotic acid, which is able to release 7 protons from the molecule. The first three pK_a values characterizing the dissociation processes were lower than 2. Therefore, in order to achieve precise values of pK_a Metrohm Biotrode was used (the electrode works properly in the pH range of 1–11). During the calculations based on the titrations data, the best matching of the experimental and calculated curves was observed in the case of the H_7L model. It can be assumed that the obtained values of the first three constants are reliable.

The comparison of acid dissociation constant values (Table 1) shows that the first deprotonation processes overlap with each other and the functional groups release protons almost simultaneously ($pK_{a2} - pK_{a1} = 0.08$). Based on an analysis of literature data on the deprotonation values of various functional groups, the three most acidic moieties are ranked in the order of increasing basic character, as follows: heterocyclic nitrogen of the pyrimidine derivative ($pK_a \approx 1.7$) [32], thiazole nitrogen ($pK_a \approx 1.8$) [33] and thiazoline nitrogen ($pK_a \approx 2.7$) [34]. Most probably, deprotonation takes place in this order within the functional groups of the phleomycin molecule. The subsequent pK_a values (6.38 and 7.12) characterize the acid-base properties of the imidazole nitrogen atom and α-NH_3^+ of β-aminoalanine, respectively [35,36]. The last two obtained values (11.19 and 11.20) refer to the simultaneous dissociation of guanidine and the amino group of 4-amino-5-methylpyrimidine [37,38].

Formation of the Cu(II)-phleomycin complex starts at a very low pH value with the stoichiometry CuH_4L^{6+} (Fig. 3). There are three very acidic groups in the phleomycin molecule. All of them have the ability to anchor copper(II) ions. However, the d–d transition appears at 610 nm in the UV–Vis spectra and at 550 nm and 683 nm in the CD spectra. The pattern of the Cotton effects is similar to numerous copper (II) complexes with peptides [40] and spectroscopic parameters suggest the involvement of only two nitrogen donor atoms in the binding process (Table 2) [39]. Most likely, one of them is the nitrogen atom of the pyrimidine ring (pK_a = 1.69, Table 1), because it is the most acidic moiety in the molecule and the other two heterocyclic nitrogen atoms are responsible for the interaction with DNA and probably do not participate in the copper ion binding process [14]. This conclusion coincides with the data obtained for the Cu(II)-bleomycin system [16,17]. Moreover, apart from the d–d transitions, the CD spectra also yield the charge transfer (CT) ones which support hypothesis that in metal ion binding process pyrimidine ring and amino group are involved (see Figs. S3 and S4 in Supplementary Information). Analysis of the coordination sphere executed by EPR spectroscopy and compared to the Peisach–Blumberg plot confirms 2 N binding mode. The observed nitrogen hyperfine couplings in the complexes are typical for equatorially coordinated ligands ($A_{||}$ = 178 G, $g_{||}$ = 2.303) [41,42]. In frozen solution EPR spectra of all the studied copper complexes showed axial symmetry ($g_{||} > > g_{\perp} > 2.0023$). This trend indicates that the unpaired electron on the copper ion is localized in the d_{x2-y2} orbital which

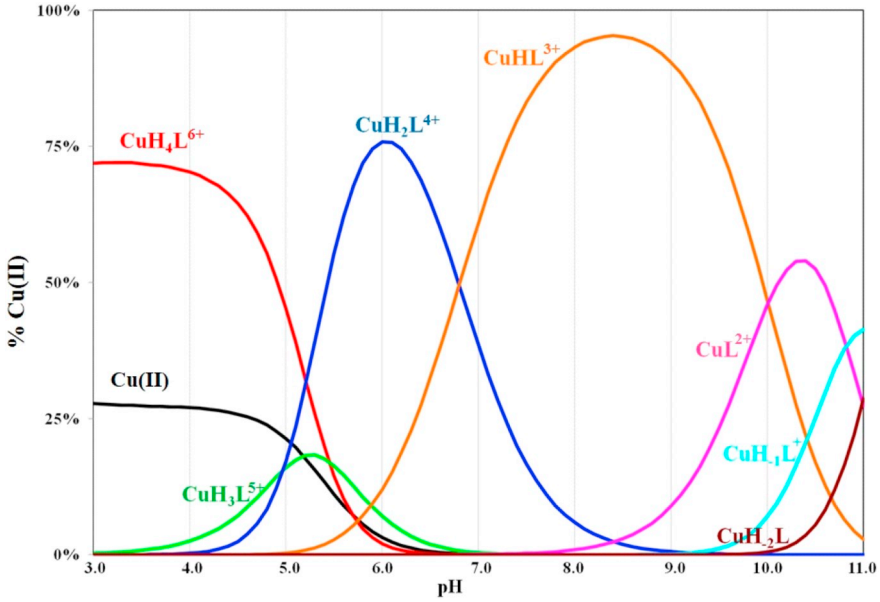

Fig. 3. Species distribution diagram for the Cu(II)-phleomycin system (M:L 1:1.1; [Cu(II)] = 1 mM).

Table 2
Stability constants and spectroscopic parameters for Cu(II)-phleomycin system.

Potentiometry			UV–Vis		CD		EPR		
Complex	logβ[a]	pK_a[b]	λ [nm]	ε [M^{-1} cm^{-1}]	λ [nm]	Δε [M^{-1} cm^{-1}]	$A_{\|\|}$ [G]	$g_{\|\|}$	$g_{\perp}$
CuH_4L^{6+}	39.74(1)	5.45	243	3844	245[c]	+0.022	178	2.303	2.061
			300	1585	273[d]	+0.021			
			610	40	550[h]	+0.071			
					683[h]	−0.024			
CuH_3L^{5+}	34.29(1)	4.97				–			
CuH_2L^{4+}	29.32(1)	6.80	243	5375	242[c]	−0.017	200	2.176	2.066
			300	2817	256[e]	+0.022			
			580	75	273[d]	+0.035			
					295[f]	+0.031			
					341[g]	−0.019			
					550[h]	+0.094			
					683[h]	−0.039			
$CuHL^{3+}$	22.52(2)	10.01	243	5420	242[c]	+0.099	180	2.201	2.069
			300	2818	258[e]	+0.026			
			600	75	273[d]	−0.049			
					310[f]	−0.068			
					341[g]	−0.027			
					602[h]	+0.135			
CuL^{2+}	12.51(3)	10.82	243	6098	242[c]	+0.021	180	2.201	2.069
			300	3127	258[e]	+0.051			
			610	77	273[d]	−0.080			
					310[f]	−0.131			
					342[g]	−0.073			
					602[h]	+0.146			
$CuH_{-1}L^{+}$	1.69(3)	11.16	243	6535	242[c]	+0.341	180	2.201	2.069
			300	3127	259[e]	+0.104			
			600	77	273[d]	−0.149			
					310[f]	−0.199			
					342[g]	−0.103			
					602[h]	+0.146			
$CuH_{-2}L$	−9.47(4)	–	243	6628	242[c]	+0.341	180	2.201	2.069
			300	3127	259[e]	+0.104			
			600	78	273[d]	−0.149			
					310[f]	−0.199			
					342[g]	−0.103			
					602[h]	+0.146			

Standard deviations on the last digit of stability constants are given in parentheses.
[a] Overall stability constants (β) expressed by the equation: $\beta(CuH_nL^{(n+2)+}) = [CuH_nL^{(n+2)+}]/[Cu^{2+}][L^{7+}][H^+]^n$).
[b] Acid dissociation constants (pK_a) expressed as: $pK_a = \log\beta(CuH_nL^{(n+2)+}) - \log\beta(CuH_{n-1}L^{(n+1)+})$.
[c] $N_{pyrimidine}$ ➔ Cu(II) charge transfer (CT).
[d] NH_2 ➔ Cu(II) CT.
[e] $N_{imidazole}$ π_2 ➔ Cu(II) CT.
[f] N^-_{amide} ➔ Cu(II) CT.
[g] $N_{imidazole}$ π_1 ➔ Cu(II) CT.
[h] d-d transition.

is usually expected for square planar, pyramidal and tetragonally elongated octahedron coordination of copper complexes [43]. There was no further splitting in the EPR spectra and superhyperfine interaction due to the isotope ^{14}N was not obtained in the perpendicular region of the Cu(II) spectra.

As far as phleomycin is concerned, the formation of the first complex species CuH_4L^{6+} is a result of the dissociation of three protons from the antibiotic molecule, with simultaneous coordination of two donor atoms. However, the thiazole and thiazoline nitrogen atoms deprotonate without participating in the coordination process. It is interesting which moiety is responsible for metal ion binding in CuH_4L^{6+}. The second donor atom is potentially the nitrogen of the secondary amine from the β-aminoalanine residue (N_2, Fig. 2). Its deprotonation was not observed in the ligand as the lone electron pair was involved in the formation of hydrogen bonds with heterocyclic nitrogen of pyrimidine and the α-amino group of β-aminoalanine (Fig. 2) [44]. However, as a result of breaking the hydrogen bond, deprotonation and coordination of the copper(II) ion by the heterocyclic nitrogen of pyrimidine (N_1, Fig. 2), the lone electron pair of the secondary amino group may possibly be involved in the formation of a coordination bond with the metal ion. The resulting five-membered chelate ring seems to be very stable. To confirm the coordination mode, the computational methods of theoretical chemistry were used as a valuable tool to predict the structure and stability of the complexes [45–47]. At the DFT level of theory we found four thermodynamically stable multiple connected metal ion-phleomycin complexes (Fig. 4).

Theoretical calculations demonstrate that the CuH_4L^{6+} complex is created by four interactions. Two nitrogens, one from the 5-methylpyrimidin-4-amine ring (N_1), the other from the secondary amino group (N_2) take part in copper binding. Both N…Cu^{2+} distances (collected in Table 3) are close to 2 Å, a typical bond length for such interactions. Interestingly, the metal-peptide complex gains additional stability with two supporting O…Cu(II) interactions, where the oxygen atoms are supplied by the carbonyl groups closest to N_1…Cu(II) and N_2…Cu(II) (O_1 and O_2, respectively).

In the CuH_4L^{6+} complex, four hydrogen bonds as shown in Fig. 5 were found. The hydrogen bonds can be divided into two groups in terms of length: three short HBs with the H…A distance < 1.8 Å (Table 4) and one significantly longer where H…O reaches 2.258 Å.

Interestingly, none of the backbone atoms of the CuH_4L^{6+} complex

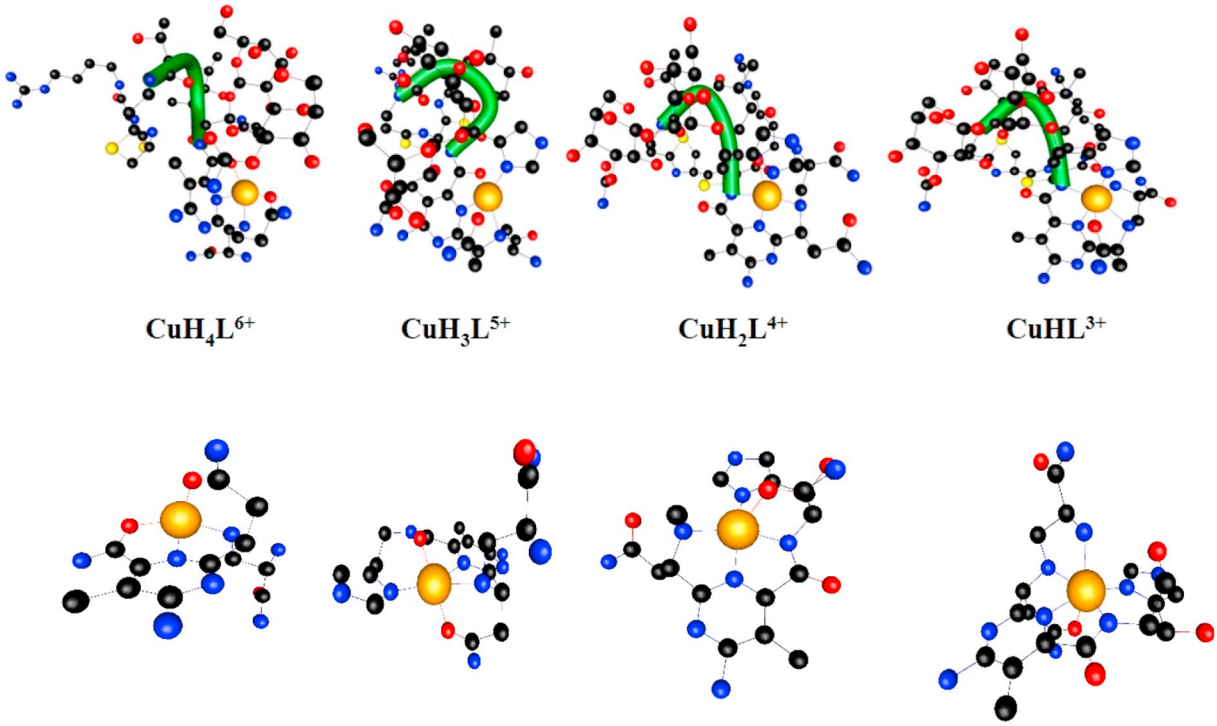

Fig. 4. The structures of phleomycin complexes with Cu(II) cation. Green tubes follow peptide backbone. Below complexes their fragments involved into metal binding.

Table 3
The Cu(II)…X distances in [Å] (index of donor atom reflect the Fig. 1).

X	CuH_4L^{6+}	CuH_3L^{5+}	CuH_2L^{4+}	$CuHL^{3+}$
Cu(II)…X				
N_1	1.999	2.030	1.983	2.023
N_2	2.056	2.030	2.095	2.010
N_3		1.989	1.989	2.024
N_4			1.977	2.238
N_5				2.276
O_1	1.972	1.997		2.408
O_2	2.019	2.014		
O_3			2.304	

Table 4
Hydrogen bonds of $ACuH_4L^{6+}$ complex.

	H...A [Å]	D-H…A [deg]	Fragment
1	1.847	176.6	N-H…O
2	1.889	162.9	O-H…O
3	1.852	155.6	N-H...O
4	2.258	160.5	N-H...O

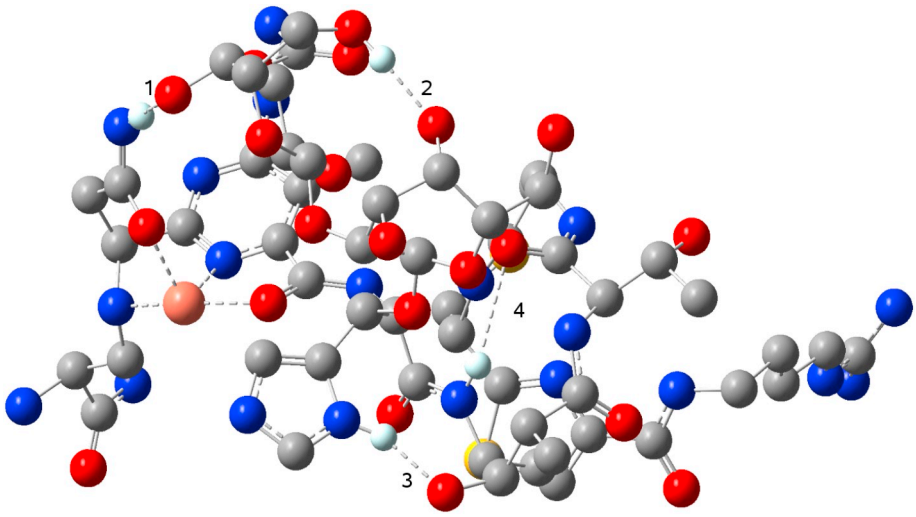

Fig. 5. The hydrogen bonds of CuH_4L^{6+} complex (only in HB involved hydrogen atoms are presented).

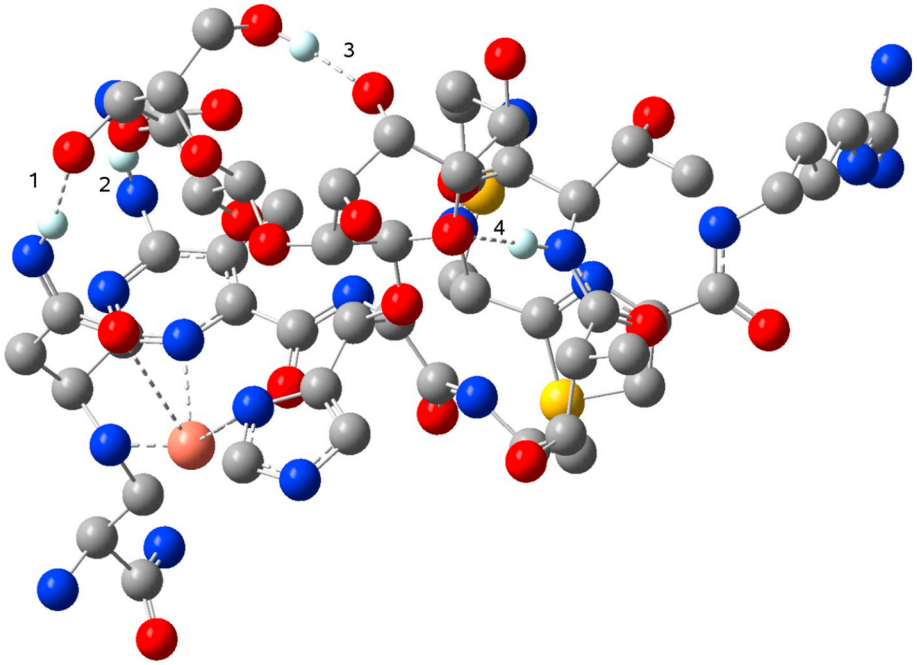

Fig. 6. The hydrogen bonds of CuH_3L^{5+} complex (only in HB involved hydrogen atoms are presented).

Table 5
Hydrogen bonds of CuH_3L^{5+} complex.

	H…A [Å]	D-H…A [deg]	Fragment
1	1.837	167.4	N-H…O
2	1.948	158.4	N-H…N
3	1.849	171.2	O-H…O
4	2.193	160.0	N-H…O

takes part in the building of the intramolecular HB system. This can be explained by the backbone length which results in the lack of backbone-backbone or backbone-side chain interactions, successfully preventing building of regular fragments of the secondary structure of the ligand.

The pK_a value of the CuH_4L^{6+} species is ca. 0.5 log units higher than that of the CuH_3L^{5+} form. Such convergence in the potentiometric calculations can be observed for simultaneous deprotonation processes. The difference smaller than 0.6 log units between the consecutive constants suggests that both species are formed at a similar pH value [48]. It is impossible to obtain the spectroscopic characteristic for the next complex that was formed, CuH_3L^{5+}, due to its low concentration and the coexistence of the CuH_4L^{6+} and CuH_2L^{4+} species (Fig. 3). Therefore, potentiometric data were used to determine the coordination sphere. The value of $\log K = \log\beta_{CuH3L} - \log\beta_{H3L}$ equal 4.78 corresponds to the monodentate coordination of Cu(II)-imidazole [49]. It suggests participation in the binding of imidazole nitrogen and the formation of a {3N} complex type. This suggestion was confirmed at the DFT level of theory. The CuH_3L^{5+} complex forms similar metal-peptide interactions as those found in CuH_4L^{6+}. However, one additional, short (1.989 Å) interaction between imidazole nitrogen (N_3) and metal cation was formed (Table 3). It is noteworthy that the imidazole-metal interaction is the shortest among all interactions found in the complex species. Three N…Cu(II) bonds are additionally supported by two O…Cu(II). Oxygen atoms originate from the very same carbonyl groups that stabilize the CuH_4L^{6+} complex. The four member system of intramolecular hydrogen bonds is presented in Fig. 6.

The additional imidazole…Cu(II) interaction which was found in CuH_3L^{5+} (and not in the CuH_4L^{6+} complex) does not influence the quantity of HBs found in CuH_4L^{6+}. The CuH_3L^{5+} complex is stabilized by four hydrogen bonds with lengths presented in Table 5. It is worthy of note that the three types: N-H…O, N-H…N and O-H…O are present in the complex, and none of backbone atoms is involved in the stabilization of the complex by hydrogen bond.

A further increase of the pH value up to around 6.0, causes a hypsochromic shift of the d-d absorption band (λ = 580 nm), which suggests the {4 N} coordination type. Moreover, on the CD spectra in the UV region such transitions are observed: $N_{pyrimidine} \rightarrow Cu(II)$, $N_{imidazole}$ $\pi_2 \rightarrow Cu(II)$, $N^-_{amide} \rightarrow Cu(II)$, $-NH_2 \rightarrow Cu(II)$ and $N_{imidazole}$ $\pi_1 \rightarrow Cu(II)$ at 242, 256, 273, 295 and 341 nm, respectively (Table 2). It suggests coordination of the above mentioned donors. From EPR results, it is concluded, that copper has a pseudo square planar coordination geometry because the observed nitrogen hyperfine couplings in the complexes are specific for equatorially coordinated four nitrogen ligands [16,17]. DFT calculations show that the CuH_2L^{4+} complex engages N_{1-3} donors in the coordination sphere, similarly to the previously described CuH_3L^{5+} species, and the cation is also connected via N_4 (Fig. 1) amide nitrogen of histidyl residue with 1.977 Å length (see Table 3). The $N_{1-4}…Cu^{2+}$ interactions are supported by one additional O_3…cation interaction that involves oxygen form the carbonyl group deriving from β-hydroxyhistidine. Moreover, the CuH_2L^{4+} complex builds the richest network of hydrogen bonds (in total 8, Fig. 7) among all investigated complexes.

The large number of HBs in CuH_2L^{4+} does not demonstrate the expected cooperative chains arrangement – only two HBs (6 and 7, as presented in Table 6) form one short chain, therefore the non-additive part of the HB stabilization of the complex is available here.

Interestingly, on the UV–Vis spectra, the formation of the $CuHL^{3+}$ complex is accompanied by a bathochromic shift of the d-d band to a wavelength of around 600 nm. Such a change in the d-d transition energy may suggest participation in the coordination process of five nitrogen atoms, with one of them being in the apical position. Although the transition energy is typical of {3N} complexes, it should be borne in mind that the nitrogen donor located in the axial position "reduces" the contribution to the transition energy of one of the nitrogen atoms coordinated in the equatorial positions [50]. The parameters of the EPR spectrum are also significantly changed. The values of $A_{||}$ = 180 G with $g_{||}$ (2.201) > $g_{\perp}$ (2.069) are characteristic for five-nitrogen donor atoms which have square-pyramidal geometry (in contrast to trigonal

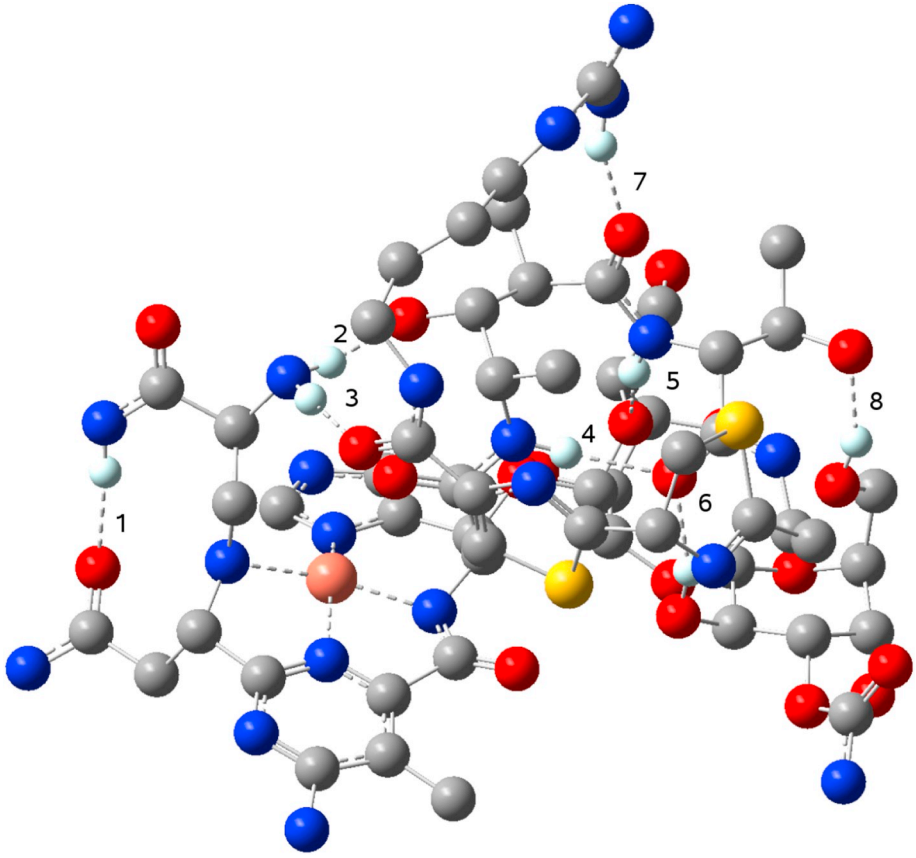

Fig. 7. The hydrogen bonds of CuH_2L^{4+} complex (only in HB involved hydrogen atoms are presented).

Table 6
Hydrogen bonds of CuH_2L^{4+} complex.

	H…A [Å]	D-H…A [deg]	Fragment
1	1.926	174.7	N-H…O
2	1.716	167.5	N-H…O
3	1.830	170.1	N-H…O
4	2.016	172.4	N-H…O
5	1.913	159.3	O-H…O
6	1.933	159.1	O-H…O
7	1.877	159.3	N-H…O
8	1.857	156.2	O-H…O

bipyramidal complexes for which $g_{\perp} > g_{||} \approx 2.00$) [51]. The p$K_a$ value accompanying the formation of this complex species is 6.80 and it is slightly lower than the proton release from the α-NH_3^+ of the β-aminoalanine residue in the free ligand. This suggests the participation of this amino group in the copper(II) binding. To confirm the coordination mode and the geometry of the complex, the DFT calculations were performed. The $CuHL^{3+}$ complex forms five nitrogen-Cu(II) interactions supported by weak carbonyl-cation interaction (2.408 Å) in O_1 position which is significantly longer than the respective O_1-Cu(II) distances found in the CuH_4L^{6+} and CuH_3L^{5+} complexes. In comparison to a {4N} complex type (CuH_2L^{4+}), an additional metal-ligand 2.276 Å interaction was found. It is worthy of note that apart from the long N_5-Cu(II) distance, also the distance between copper cation and N_5 in the 5 N complex is significantly longer in comparison with the very same interaction we found in the 4N complex (Table 3).

The hydrogen bonds network presented in Fig. 8 contains seven HBs that come exclusively from the side chains.

Hydrogen bonds lengths of the $CuHL^{3+}$ complex are collected in Table 7. Among seven HBs, a short cooperative chain (consisting of HB 2 and 3) was found. It is worthy of note that for all the investigated complexes only three types of HB were found, namely N-H…O, O-H…O and N-H…N.

The copper binding area involves a rather small region of the molecule, which is additionally well separated from the phleomycin part responsible for the interaction with DNA as shown in Fig. 9. However, it can also be seen that a metal ion is relatively close to the nucleic acid binding moiety. This supports the hypothesis that copper ion is important in the anticancer activity which involves DNA degradation.

While analyzing the set of spectroscopic parameters characterizing the complex species from $CuHL^{3+}$ to $CuH_{-2}L$, it can clearly be seen that they do not change (Table 2). Their constancy, despite the increase of the pH value of the solution and dissociation of successive protons of the phleomycin molecule, proves that the coordination sphere of the metal ion remains unchanged. Therefore, an increase of the pH does not cause changes in the coordination sphere of the cupric ion. Only the deprotonation of subsequent moieties, guanidine and amino group, in position 4 of the pyrimidine ring is observed. It takes place in the same order as in the case of an uncomplexed antibiotic. The last pK_a value (11.16) which accompanies the formation of the $CuH_{-2}L$ form can be attributed to the deprotonation of a water molecule coordinated by the Cu(II) ion [52].

The anticancer mode of action of phleomycin is considered to be based on the DNA cleavage in the presence of molecular oxygen [53]. However, the complex is not an efficient catalyst of the cleavage of plasmid DNA in the absence of any added cofactors (Fig. 10). The ability to mediate both single-stranded and double-stranded DNA damage requires the presence of a one-electron reductant, such as dithiothreitol, glutathione, 2-mercaptoethanol or ascorbic acid. The maximum rate of degradation of the supercoiled plasmid DNA form, which leads to the formation of linear form III, was observed in the presence of 1 mM ascorbic acid (lane 11). Ascorbic acid as well as

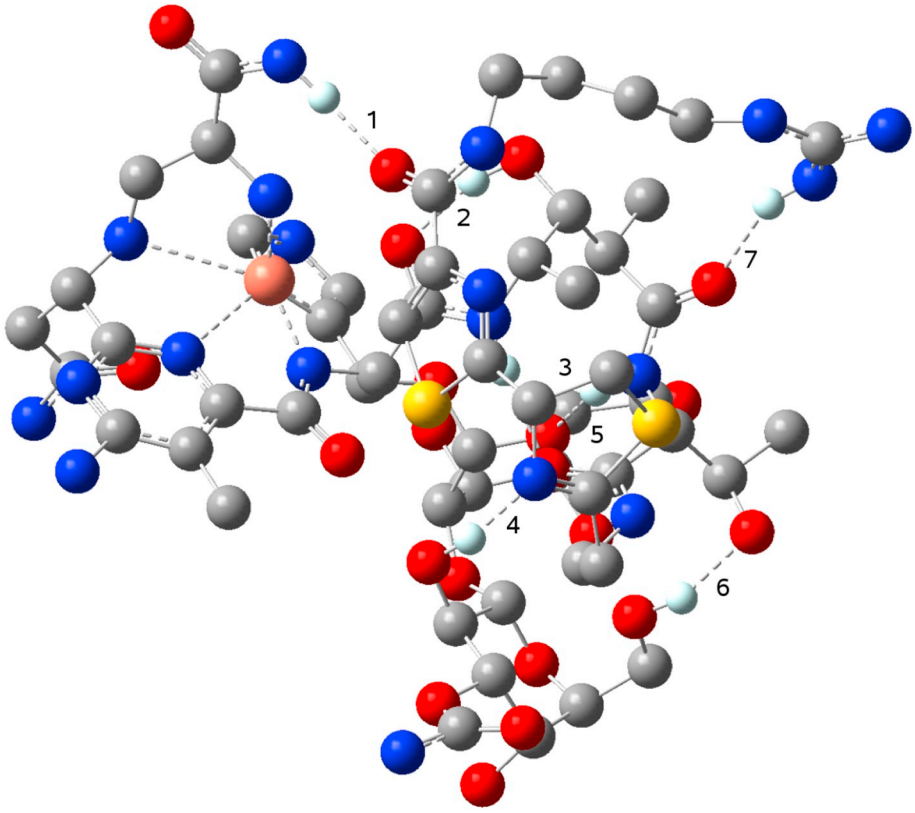

Fig. 8. The hydrogen bonds of $CuHL^{3+}$ complex (only in HB involved hydrogen atoms are presented).

Table 7
Hydrogen bonds of $CuHL^{3+}$ complex.

	H...A [Å]	D-H…A [deg]	Fragment
1	1.925	164.4	N-H...O
2	1.799	159.2	O-H...O
3	2.000	165.1	N-H...O
4	1.974	158.3	O-H...O
5	1.977	152.7	N-H...O
6	1.828	156.5	O-H...O
7	1.920	152.6	N-H...O

dithiothreitol, glutathione and 2-mercaptoethanol may reduce Cu(II) to Cu(I) and therefore lead to the formation of reactive oxygen species (ROS) and DNA degradation [54–57]. It is worth noting that phleomycin is also active in the presence of hydrogen peroxide, which is both an oxidizing and reducing agent. In the case of copper(II) complexes with peptides, production of reactive oxygen species (ROS) via the Fenton-like reaction mechanism is often observed. In the first step, Cu (II) is reduced to Cu(I) by H_2O_2 with simultaneous formation of a superoxide radical anion. In the next step, Cu(I) reacts with H_2O_2 and produces OH^-, ·OH and Cu(III) [58].

As was seen in the previous figure only plasmid linearization, but not further degradation to short DNA fragments, was observed in this experiment. Due to the fact that the most powerful cleaving system is phleomycin in the presence of ascorbic acid the reaction kinetics was followed (Fig. 11). It demonstrates the gradual degradation of superhelical DNA to its linear form. Nicking process is based on the accumulation of single-strand scissions, which finally results in double-strand cleavages. The stepwise mechanism is clearly seen at lanes 3–7. It is supported by the interdependence of form I decrease with simultaneous increase of form II. After complete disappearance of superhelical form which is completely converted to form II (lane 6), we observe a small amount of form III which increases in time dependent manner. It suggests that the DNA fragmentation is a result of accumulation of random single strand breaks in the plasmid, rather than the immediate formation of double strand breaks which was proposed

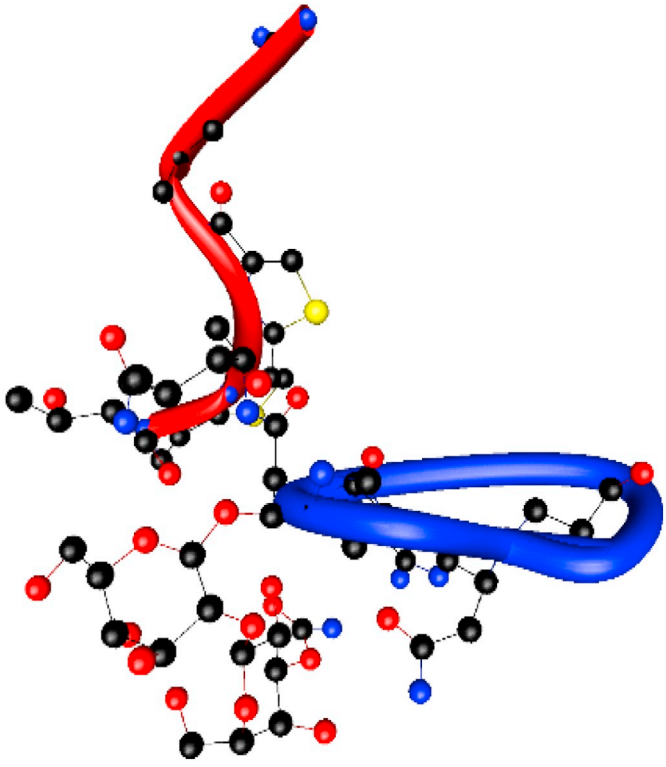

Fig. 9. The binding areas: blue dedicated for Cu(II), red for DNA.

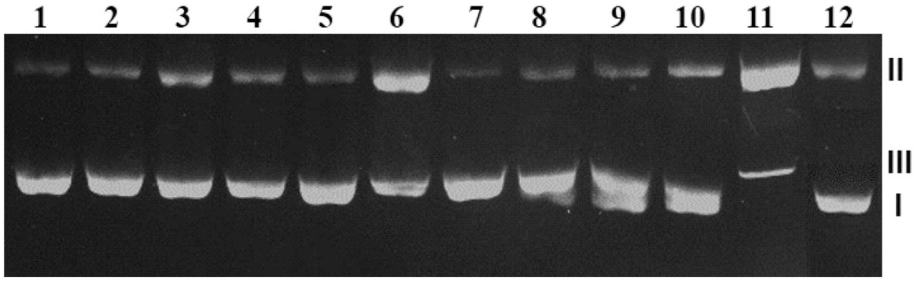

Fig. 10. Plasmid DNA degradation in the presence of 0.01 mM phleomycin and different cofactors in a buffer solution at pH 7.4.
Lane 1. Plasmid; **lane 2.** plasmid + phleomycin; **lane 3.** plasmid + phleomycin + H_2O_2 (1 mM); **lane 4.** plasmid + phleomycin + H_2O_2 (0.1 mM); **lane 5.** plasmid + phleomycin + DTT (1 mM); **lane 6.** plasmid + phleomycin + DTT (0.1 mM); **lane 7.** plasmid + phleomycin + mercaptoethanol (1 mM); **lane 8.** plasmid + phleomycin + mercaptoethanol (0.1 mM); **lane 9.** plasmid + phleomycin + GSH (1 mM); **lane 10.** plasmid + phleomycin + GSH (0.1 mM); **lane 11.** plasmid + phleomycin + ascorbic acid (1 mM); **lane 12.** plasmid + phleomycin + ascorbic acid (0.1 mM).

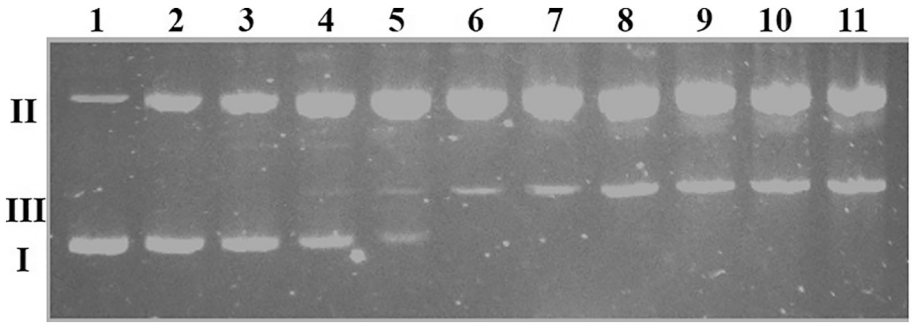

Fig. 11. Kinetics of pBR322 plasmid cleavage in the presence of 0.01 mM phleomycin and 1 mM ascorbic acid at pH 7.4.
Lanes 1–11. system incubated during 0, 5, 10, 20, 30, 45, 60, 75, 90, 105, 120 min., respectively.

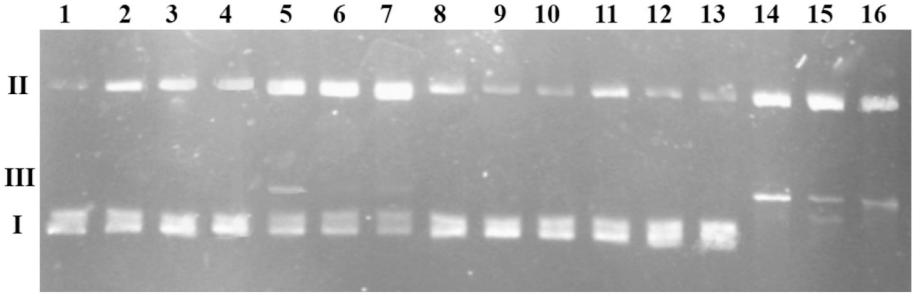

Fig. 12. Agarose gel electrophoresis of plasmid DNA cleavage by phleomycin and cofactors in the presence of scavengers (DMSO and NaN_3) at pH 7.4.
Lane 1. plasmid; **lane 2.** plasmid + phleomycin (0.01 mM) + H_2O_2 (1 mM); **lane 3.** plasmid + phleomycin (0.01 mM) + H_2O_2 (1 mM) + DMSO (1.4 M); **lane 4.** plasmid + phleomycin (0.01 mM) + H_2O_2 (1 mM) + NaN_3 (40 mM); **lane 5.** plasmid + phleomycin + DTT (1 mM); **lane 6.** plasmid + phleomycin + DTT (1 mM) + DMSO (1.4 M); **lane 7.** plasmid + phleomycin + DTT (1 mM) + NaN_3 (40 mM); **lane 8.** plasmid + phleomycin + mercaptoethanol (1 mM); **lane 9.** plasmid + phleomycin + mercaptoethanol (1 mM) + DMSO (1.4 M); **lane 10.** plasmid + phleomycin + mercaptoethanol (1 mM) + NaN_3 (40 mM); **lane 11.** plasmid + phleomycin + GSH (1 mM); **lane 12.** plasmid + phleomycin + GSH (1 mM) + DMSO (1.4 M); **lane 13.** plasmid + phleomycin + GSH (1 mM) + NaN_3 (40 mM); **lane 14.** plasmid + phleomycin + ascorbic acid (1 mM); **lane 15.** plasmid + phleomycin + ascorbic acid (1 mM) + DMSO (1.4 M); **lane 16.** plasmid + phleomycin + ascorbic acid (1 mM) + NaN_3 (40 mM).

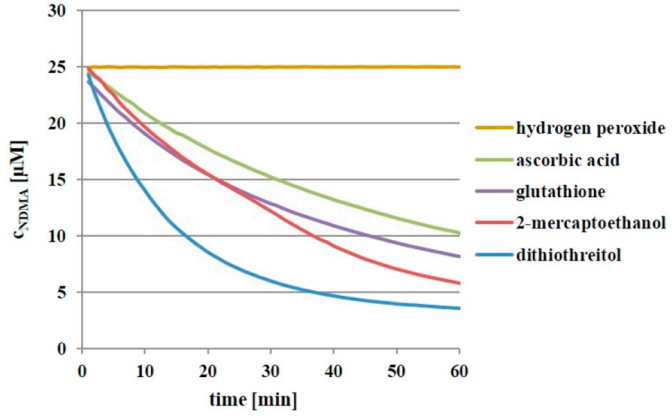

Fig. 13. NDMA decomposition in the presence of 0.01 mM phleomycin and listed cofactors.

Table 8
The pseudo-first order rate constants $k_{obs} \times 10^{-2}$ [s^{-1}] for NDMA (25 μM) decomposition in the presence of 0.01 mM phleomycin and 1 mM cofactors at pH 7.4 and 37 °C.

Cofactor	$k_{obs} \times 10^{-2}$ [s^{-1}]
H_2O_2	–
ascorbic acid	1.73(1)
glutathione	2.26(2)
2-mercaptoethanol	2.52(2)
dithiothreitol	5.48(8)

previously for Cu(II) aqua ion interacting with DNA [59,60].

In order to determine whether reactive oxygen species were present in the studied systems, appropriate scavengers: DMSO (1.4 M) for ·OH and NaN_3 (40 mM) for singlet oxygen were added to the reaction mixture before addition of the complex [61]. It can be easily seen in

Fig. 12 that in the case of phleomycin in the presence of ascorbic acid and thiol cofactors, hydroxyl radical and singlet oxygen were formed. The amount of cleaved DNA form in the case of used scavengers is lower than for appropriate control reaction (compare lane 5 with 6 and 7, lane 8 with 9 and 10, lane 11 with 12, 13 and lane 14 with 15, 16). However, addition of DMSO to the phleomycin-H_2O_2 system had an insignificant effect, which suggests that negligible amounts of ·OH were generated (lane 2–4). It should be noted here that the control sample with H_2O_2, DMSO and NaN_3 did not cause any DNA degradation (data not shown).

To calculate rate constants of hydroxyl radical formation, UV–Vis spectroscopy with reporting molecule (NDMA) was applied. The rate of NDMA decomposition (Fig. 13) showed that the phleomycin-dithiothreitol system produces the highest amount of ·OH. An analysis of the shapes of the curves demonstrated that the NDMA degradation initially followed the pseudo-first order kinetics, but with the passage of time (after 10 min.), the rates of the ROS generation changed their dynamics (Fig. 10). Those observations were common for all studied systems. The calculated kinetic parameters are collected in Table 8.

4. Conclusions

The full characteristic of the coordination process of phleomycin was possible through combined experimental and computational methods. Calculations based on the potentiometric titrations allowed the acid–base characteristics of the ligand and the determination of the overall stability constants and the stoichiometry of the complex species. The determination of donor atoms was based on computational and spectroscopic methods, such as UV–Vis and EPR. As the last step, a three-dimensional structure was obtained. It was concluded that the following donor atoms are involved in copper(II) ions coordination by a phleomycin molecule: heterocyclic N_1 (Fig. 1) nitrogen deriving from the pyrimidine ring, secondary amine of β-aminoalanine (N_2), imidazole (N_3) and amide of the nearest peptide bond (N_4 from β-hydroxyhistidine) similar to many other peptides [62]. However, also the α-amino functional group of β-aminoalanine (N_5) is engaged in the metal ion binding process. This group is coordinated in the axial position. As a result of this coordination type, four thermodynamically stable chelate rings are formed: three five-membered and one six-membered. The complex has a square-pyramidal geometry. All studied species build networks (4–8) of hydrogen bonds that additionally stabilize the complexes. The structure of the HB network prefers only side chain atoms that display small or no cooperativity impact on the complexes. It is worth mentioning that all studied complexes display two separated, well defined regions responsible for the interaction between DNA and cations.

Phleomycin itself is not an effective DNA-cleaving agent. However, it has the ability to promote DNA degradation in the presence of cofactors which may reduce copper(II) ions. Among all the studied compounds, ascorbic acid seems to be the most powerful agent and it leads to double-stranded DNA cleavage. Numerous reactive oxygen species are involved in the degradation of nucleic acid, e.g. hydroxyl radical. The ·OH formation is most efficient when dithiothreitol is used. After 60 min. Incubation at 37 °C in the presence of phleomycin and DTT, almost 85% of NDMA was decomposed what means that large amounts of hydroxyl radical are generated in the studied system.

Acknowledgements

The research was supported by financed from the Polish National Science Centre (Grant NCN 2014/13/B/ST5/04359).

Appendix A. Supplementary data

Supplementary data to this article can be found online at https://doi.org/10.1016/j.jinorgbio.2019.03.010.

References

[1] A. Jemal, F. Bray, M.M. Center, J. Ferlay, M.E. Ward, D. Forman, Global cancer statistics, CA Cancer J. Clin. 61 (2011) 69–90, https://doi.org/10.3322/caac.20107.
[2] L.A. Torre, F. Bray, R.L. Siegel, J. Ferlay, J. Lortet, Tieulent, A. Jemal, Global cancer statistics, 2012, CA Cancer J. Clin. 65 (2015) 87–108, https://doi.org/10.3322/caac.21262.
[3] World Health Organization, Cancer, http://www.who.int/cancer/en/, (2018) , Accessed date: 13 September 2018.
[4] World Health Organization, Key Statistics, http://www.who.int/cancer/resources/keyfacts/en/, (2018) , Accessed date: 13 September 2018.
[5] M. Rugge, M. Fassan, D. Graham, V.E. Strong, et al. (Ed.), Epidemiology of gastric Cancer, Springer, Cham, New York, 2015, pp. 23–32.
[6] S. Bullman, C.S. Pedamallu, E. Sicinska, T. Clancy, S. Ogino, J. Tabernero, C. Fuchs, W.C. Hahn, P. Nuciforo, M. Meyerson, Abstract 5129: fusobacterium and co-occurring microbes in primary and metastatic colorectal cancer, Cancer Res. 78 (2018) 5129, https://doi.org/10.1158/1538-7445.AM2018-5129.
[7] R. Misra, S. Acharya, S.K. Sahoo, Cancer nanotechnology: application of nanotechnology in cancer therapy, Drug Discov. Today 15 (2010) 842–850, https://doi.org/10.1016/j.drudis.2010.08.006.
[8] L.-J. Ming, Structure and function of "metalloantibiotics", Med. Res. Rev. 23 (2003) 697–762, https://doi.org/10.1002/med.10052.
[9] M. Jeżowska-Bojczuk, K. Stokowa-Sołtys, Peptides having antimicrobial activity and their complexes with transition metal ions, Eur. J. Med. Chem. 143 (2018) 997–1009.
[10] J.C. Dabrowiak, F.T. Greenaway, W.E. Longo, M. Van Husen, S.T. Crooke, A spectroscopic investigation of the metal binding site of bleomycin A2. The Cu(II) and Zn (II) derivatives, Biochim. Biophys. Acta, Nucleic Acids Protein Synth. 517 (1978) 517–526, https://doi.org/10.1016/0005-2787(78)90218-6.
[11] J. Stubbe, J.W. Kozarich, Mechanisms of bleomycin-induced DNA degradation, Chem. Rev. 87 (1987) 1107–1136, https://doi.org/10.1021/cr00081a011.
[12] T.E. Lehmann, M.L. Serrano, L. Que, Coordination chemistry of Co(II)-bleomycin: its investigation through NMR and molecular dynamics, Biochemistry 39 (2000) 3886–3898, https://doi.org/10.1021/bi991841p.
[13] S. Ida, K. Iwamaru, M. Fujita, Y. Okamoto, Y. Kudo, H. Kurosaki, M. Otsuka, l-Histidyl-glycyl-glycyl-l-histidine. Amino-acid structuring of the bleomycin-type pentadentate metal-binding environment capable of efficient double-strand cleavage of plasmid DNA, Bioorg. Chem. 62 (2015) 8–14, https://doi.org/10.1016/j.bioorg.2015.06.007.
[14] M. Sugiyama, T. Kumagai, M. Hayashida, M. Maruyama, Y. Matoba, The 1.6-Å crystal structure of the copper(II)-bound bleomycin complexed with the bleomycin-binding protein from bleomycin-producing Streptomyces verticillus, J. Biol. Chem. 277 (2002) 2311–2320, https://doi.org/10.1074/jbc.M103278200.
[15] L.F. Povirk, M. Hogan, N. Dattagupta, M. Buechner, Copper(II). bleomycin, iron (III).bleomycin, and copper(II).phleomycin: comparative study of deoxyribonucleic acid binding, Biochemistry 20 (1981) 665–670, https://doi.org/10.1021/bi00506a034.
[16] J.P. Albertini, A. Garnier-Suillerot, Formation of copper-bleomycin complexes: evidence of a three-step process, J. Inorg. Biochem. 25 (1985) 15–24, https://doi.org/10.1016/0162-0134(85)83003-8.
[17] E. Kimura, H. Kurosaki, Y. Kurogi, M. Shionoya, M. Shiro, pH-dependent coordination mode of new bleomycin synthetic analogs with copper(II), iron(II), and zinc(II), Inorg. Chem. 31 (1992) 4314–4321, https://doi.org/10.1021/ic00047a019.
[18] K.E. Loeb, J.M. Zaleski, C.D. Hess, S.M. Hecht, E.I. Solomon, Spectroscopic investigation of the metal ligation and reactivity of the ferrous active sites of bleomycin and bleomycin derivatives, J. Am. Chem. Soc. 120 (1998) 1249–1259, https://doi.org/10.1021/ja971839q.
[19] D. Solaiman, E.A. Rao, W. Antholine, D.H. Petering, Properties of the binding of copper by bleomycin, J. Inorg. Biochem. 12 (1980) 201–220, https://doi.org/10.1016/S0162-0134(00)80202-0.
[20] Y. Iitaka, H. Nakamura, T. Nakatoni, Y. Murauka, A. Fujii, T. Takita, H. Umezawa, Chemistry of bleomycin. XX. The X-ray structure determination of P-3A Cu(II)-complex a biosynthetic intermediate of bleomycin, J. Antibiot. 31 (1978) 1070–1072, https://doi.org/10.7164/antibiotics.31.1070.
[21] K.S. Jain, T.S. Chitre, P.B. Miniyar, M.K. Kathiravan, V.S. Bendre, V.S. Veer, S.R. Shahane, C.J. Shishoo, Biological and medicinal significance of pyrimidines, Curr. Sci. 90 (2006) 793–803.
[22] K. Oda, Y. Matoba, M. Noda, T. Kumagai, M. Sugiyama, Catalytic mechanism of bleomycin N-acetyltransferase proposed on the basis of its crystal structure, J. Biol. Chem. 285 (2010) 1446–1456, https://doi.org/10.1074/jbc.M109.022277.
[23] J. Gu, R. Codd, Copper(II)-based metal affinity chromatography for the isolation of the anticancer agent bleomycin from Streptomyces verticillus culture, J. Inorg. Biochem. 115 (2012) 198–203, https://doi.org/10.1016/j.jinorgbio.2012.01.015.
[24] P. Gans, A. Sabatini, A. Vacca, SUPERQUAD: an improved general program for computation of formation constants from potentiometric data, J. Chem. Soc. Dalton Trans. (6) (1985) 1195–1200, https://doi.org/10.1039/dt9850001195.
[25] R. Cammi, Molecular Response Functions for the Polarizable Continuum Model. Physical basis and quantum mechanical formalism, in: G. Maroulis (Ed.), SpringerBriefs in Molecular Science, New York, 2013, pp. 58–70.
[26] Gaussian 09, M.J. Frisch, G.W. Trucks, H.B. Schlegel, G.E. Scuseria, M.A. Robb, J.R. Cheeseman, G. Scalmani, V. Barone, B. Mennucci, G.A. Petersson, H. Nakatsuji, M. Caricato, X. Li, H.P. Hratchian, A.F. Izmaylov, J. Bloino, G. Zheng, J.L. Sonnenberg, M. Hada, M. Ehara, K. Toyota, R. Fukuda, J. Hasegawa, M. Ishida,

T. Nakajima, Y. Honda, O. Kitao, H. Nakai, T. Vreven, J.A. Montgomery Jr., J.E. Peralta, F. Ogliaro, M. Bearpark, J.J. Heyd, E. Brothers, K.N. Kudin, V.N. Staroverov, R. Kobayashi, J. Normand, K. Raghavachari, A. Rendell, J.C. Burant, S.S. Iyengar, J. Tomasi, M. Cossi, N. Rega, J.M. Millam, M. Klene, J.E. Knox, J.B. Cross, V. Bakken, C. Adamo, J. Jaramillo, R. Gomperts, R.E. Stratmann, O. Yazyev, A.J. Austin, R. Cammi, C. Pomelli, J.W. Ochterski, R.L. Martin, K. Morokuma, V.G. Zakrzewski, G.A. Voth, P. Salvador, J.J. Dannenberg, S. Dapprich, A.D. Daniels, Ö. Farkas, J.B. Foresman, J.V. Ortiz, J. Cioslowski, D.J. Fox, Gaussian, Inc., Wallingford CT, Revision, (2009).

[27] Y. Zhao, D.G. Truhlar, The M06 suite of density functionals for main group thermochemistry, thermochemical kinetics, noncovalent interactions, excited states, and transition elements: two new functionals and systematic testing of four M06-class functionals and 12 other functionals, Theor. Chem. Accounts 120 (2008) 215–241, https://doi.org/10.1007/s00214-007-0310-x.

[28] K. Maeda, H. Kosaka, K. Yagishita, H. Umezawa, A new antibiotic, phleomycin, J. Antibiot 9A (1956) 82–85.

[29] Sigma-Aldrich Certificate of Analysis, LOT BCBF3312V, https://www.sigmaaldrich.com/catalog/CertOfAnalysisPage.do?symbol=P9564&LotNo=BCBF3312V&brandTest=SIGMA&returnUrl=%2Fproduct%2FSIGMA%2FP9564 , Accessed date: 1 September 2017.

[30] V.B. Kenche, I. Zawisza, C.L. Masters, W. Bal, K.J. Barnham, S.C. Drew, Mixed ligand Cu2+ complexes of a model therapeutic with Alzheimer's amyloid-beta peptide and monoamine neurotransmitters, Inorg. Chem. 52 (2013) 4303–4318, https://doi.org/10.1021/ic302289r.

[31] T. Nukada, A. Berces, D.M. Whitfield, Can the stereochemical outcome of glycosylation reactions be controlled by the conformational preferences of the glycosyl donor? Carbohydr. Res. 337 (2002) 765–774, https://doi.org/10.1016/S0008-6215(02)00043-5.

[32] G. Tresoldi, S. Di Pietro, D. Drommi, S. Lanza, Fluxional rearrangement in congested ruthenium(II) complexes containing pyrimidine- and/or pyridine-based dithioether ligands, Transit. Met. Chem. 35 (2010) 151–158, https://doi.org/10.1007/s11243-009-9308-7.

[33] C. Kistayya, N. G. Raghavendra Rao, B. Sanjeev Nayak, V.N. Sonar, Synthesis and evalution of antibacterial activity of some 2-amino/substituted amino-4-(phenyl/p-chlorophenyl) thiazoles, J. adv. sci. res., 4 (2013), 1–5.

[34] Z.-X. Huang, H.S. Al-Falahi, A. Cole, J.R. Duffield, C. Furnival, D.C. Jones, P.M. May, G.L. Smith, D.R. Williams, Potentiometric investigation of sparingly soluble metal-ligand systems using metal-ion buffers, Polyhedron 1 (1982) 153–155, https://doi.org/10.1016/S0277-5387(00)80977-8.

[35] M.M.A. Mohamed, M.M. Shoukry, Complex formation equilibria of palladium(II) complexes involving N,N′-dimethylethylenediamine, DNA constituents and cyclobutane dicarboxylic acid. The catalysis of glycine methyl ester hydrolysis through complex formation, Polyhedron 21 (2002) 167–173, https://doi.org/10.1016/S0277-5387(01)00958-5.

[36] J. Torres, C. Kremer, E. Kremer, H. Pardo, L. Suescun, A. Mombru, S. Dominguez, A. Mederos, R. Herbst-Irmer, J.M. Arrieta, Sm(III) complexation with α-amino acids: X-ray crystal structure of [Sm2(Hala)4(H2O)8] (ClO4)4(Cl)2, J. Chem. Soc. Dalton Trans. (2002) 4035–4041, https://doi.org/10.1016/S0925-8388(01)00979-3.

[37] S. Zhu, A. Matilla, J.M. Tercero, V. Vijaragavan, J.A. Walmsley, Binding of palladium(II) complexes to guanine, guanosine or guanosine 5′-monophosphate in aqueous solution: potentiometric and NMR studies, Inorg. Chim. Acta 357 (2004) 411–420, https://doi.org/10.1016/j.ica.2003.06.009.

[38] T. Mehdoui, J.-C. Berthet, P. Thuery, M. Ephritikhine, Lanthanide(III)/actinide(III) differentiation in coordination of azine molecules to tris(cyclopentadienyl) complexes of cerium and uranium, Dalton Trans. (2004) 579–590, https://doi.org/10.1039/b313992a.

[39] J. Brasuń, C. Gabbiani, M. Ginanneschi, L. Messori, M. Orfei, J. Świątek-Kozłowska, The copper(II) binding properties of the cyclic peptide c(HGHK), J. Inorg. Biochem. 98 (2004) 2016–2021, https://doi.org/10.1016/j.jinorgbio.2004.09.007.

[40] J. Nagaj, K. Stokowa-Sołtys, I. Zawisza, M. Jeżowska-Bojczuk, A. Bonna, W. Bal, Selective control of Cu(II) complex stability in histidine peptides by β-alanine, J. Inorg. Biochem. 119 (2013) 85–89, https://doi.org/10.1016/j.jinorgbio.2011.06.002.

[41] J. Peisach, W.E. Blumberg, Structural implications derived from the analysis of electron paramagnetic resonance spectra of natural and artificial copper proteins, Arch. Biochem. Biophys. 165 (1974) 691–708, https://doi.org/10.1016/0003-9861(74)90298-7.

[42] C. E. Jones, S.R. Abdelraheim, D.R. Brown, J.H. Viles, Preferential cu^{2+} coordination by His96 and His111 induces β-sheet formation in the unstructured Amyloidogenic region of the prion protein, J. Biol. Chem., 279 (2004), 32018–32027. DOI: https://doi.org/10.1074/jbc.M403467200.

[43] B.J. Hathaway, A.A.G. Tomlinson, Copper(II) ammonia complexes, Coord. Chem. Rev. 5 (1970) 1–43, https://doi.org/10.1016/S0010-8545(00)80073-9.

[44] N. Gupta, H. Linschitz, Hydrogen-bonding and protonation effects in electrochemistry of Quinones in aprotic solvents, J. Am. Chem. Soc. 119 (1997) 6384–6391, https://doi.org/10.1021/ja970028j.

[45] M. Wierzejewska, R. Wieczorek, Infrared matrix isolation and ab initio studies on isothiocyanic acid HNCS and its complexes with nitrogen and xenon, Chem. Phys. 287 (2003) 169–181, https://doi.org/10.1016/S0301-0104(02)00989-8.

[46] Z. Latajka, Z. Mielke, A. Olbert-Majkut, R. Wieczorek, K.G. Tokhadze, Abinitio calculations and matrix infrared spectra of the nitrous acid complexes with HF and HCl, Phys. Chem. Chem. Phys., 1 (1999), 1, 2441–2448. DOI: https://doi.org/10.1039/A900704K.

[47] E. Gumienna-Kontecka, G. Berthon, I.O. Fritsky, R. Wieczorek, Z. Latajka, H. Kozlowski, J. Chem. Soc. Dalton Trans. 0 (2000) 4201–4208, https://doi.org/10.1039/B004432F.

[48] B. Noszal, in: K. Burger (Ed.), Coordination Equilibria in Biological Active Systems, Acid–Base Properties of Bioligands in Biocoordination Chemistry, Ellis Horwood, Chichester 1990, 18–55.

[49] P. Stańczak, M. Łuczkowski, P. Juszczyk, Z. Grzonka, H. Kozłowski, Interactions of Cu^{2+} ions with chicken prion tandem repeats, Dalton Trans. 21 (2004) 2102–2107, https://doi.org/10.1039/B405753H.

[50] H. Sigel, R.B. Martin, Coordinating properties of the amide bond. Stability and structure of metal ion complexes of peptides and related ligands, Chem. Rev. 82 (1982) 385–426, https://doi.org/10.1021/cr00050a003.

[51] R.P. John, A. Sreekanth, M.R.P. Kurup, A. Usman, A.R. Ibrahim, H.-K. Fun, Spectral studies and structure of a 2-hydroxyacetophenone 3-hexamethyleneiminyl thiosemicarbazonate(−2) copper(II) complex containing 1,10-phenanthroline, Spectrochim. Acta A Mol. Biomol. Spectrosc. 59 (2003) 1349–1358, https://doi.org/10.1016/S1386-1425(02)00332-3.

[52] K.B. Szpakolski, K. Latham, C.J. Rix, J.M. White, B. Moubaraki, K.S. Murray, Synthetic and structural studies on copper 1H-[1,10]-Phenanthrolin-2-one coordination complexes: isolation of a novel intermediate during 1,10-Phenanthroline hydroxylation, Chem. Eur. J. 16 (2010) 1691–1696, https://doi.org/10.1002/chem.200901720.

[53] Sidney M. Hecht, Bleomycin: new perspectives on the mechanism of action, J. Nat. Prod. 63 (2000) 158–168, https://doi.org/10.1021/np990549f.

[54] S. Saha, M.N. Roy, Encapsulation of vitamin C into β-cyclodextrin for advanced and regulatory release, InTech, in: A.H. Hamza (Ed.), Vitamin C, Rijeka, 2017, pp. 129–145.

[55] A. Krężel, W. Leśniak, M. Jeżowska-Bojczuk, P. Młynarz, J. Brasuń, H. Kozłowski, W. Bal, Coordination of heavy metals by dithiothreitol, a commonly used thiol group protectant, J. Inorg. Biochem. 84 (2001) 77–88, https://doi.org/10.1016/S0162-0134(00)00212-9.

[56] S.-N. Yin, Y. Liu, C. Zhou, S. Yang, Glutathione-mediated Cu(I)/Cu(II) complexes: valence-dependent effects on clearance and in vivo imaging application, Nanomaterials 7 (2017) 132–142, https://doi.org/10.3390/nano7060132.

[57] S. Anbu, M. Kandaswamy, P. Suthakaran, V. Murugan, B. Varghese, Structural, magnetic, electrochemical, catalytic, DNA binding and cleavage studies of new macrocyclic binuclear copper(II) complexes, J. Inorg. Biochem. 103 (2009) 401–410, https://doi.org/10.1016/j.jinorgbio.2008.12.013.

[58] H.-J. Lee, H. Lee, C. Lee, Degradation of diclofenac and carbamazepine by the copper(II)-catalyzed dark and photo-assisted Fenton-like systems, Chem. Eng. J. 245 (2014) 258–264, https://doi.org/10.1016/j.cej.2014.02.037.

[59] K. Yamamoto, S. Kawanishi, Hydroxyl free radical is not the main active species in site-specific DNA damage induced by copper (II) ion and hydrogen peroxide, J. Biol. Chem. 264 (1989) 15435–15440.

[60] S. Oikawa, S. Kawanishi, Site-specific DNA damage induced by NADH in the presence of copper (II): role of active oxygen species, Biochemistry 35 (1996) 4584–4590, https://doi.org/10.1021/bi9527000.

[61] L.-N. Zhu, S. Shi, L. Yang, M. Zhang, K.-K. Liu, L.-N. Zhang, Water soluble cationic porphyrin TMPipEOPP-induced G-quadruplex and double-stranded DNA photocleavage and cell phototoxicity, RSC Adv. 6 (2016) 13080–13087, https://doi.org/10.1039/C5RA24964C.

[62] K. Stokowa, W. Szczepanik, N. Gaggelli, E. Gaggelli, G. Valensin, M. Jeżowska-Bojczuk, Capreomycin - a polypeptide antitubercular antibiotic with unusual binding properties toward copper(II), J. Inorg. Biochem. 106 (2012) 111–116, https://doi.org/10.1016/j.jinorgbio.2011.08.021.